

## Proton Release upon Glutathione Binding to Glutathione Transferase P1-1: Kinetic Analysis of a Multistep Glutathione Binding Process<sup>†</sup>

Anna Maria Caccuri,<sup>‡</sup> Mario Lo Bello,<sup>‡</sup> Marzia Nuccetelli,<sup>‡</sup> Maria Nicotra,<sup>‡</sup> Paola Rossi,<sup>§</sup> Giovanni Antonini,<sup>§</sup> Giorgio Federici,<sup>||</sup> and Giorgio Ricci<sup>\*,‡</sup>

Department of Biology, University of Rome "Tor Vergata", Rome, Italy, Department of Pure and Applied Biology, University of L'Aquila, L'Aquila, and Department of Biochemical Sciences, University of Rome "La Sapienza", Rome, Italy, and Children's Hospital IRCCS "Bambin Gesù", Rome, Italy

Received August 4, 1997; Revised Manuscript Received December 3, 1997

**ABSTRACT:** The fate of the thiol proton coming from the ionization of the sulfhydryl group of GSH in the active site of glutathione transferase P1-1 has been studied. pH changes caused by the binding of GSH to the enzyme in the absence of any inorganic buffer indicate that the thiol proton leaves the active site when the binary complex is formed. The amount of protons released is stoichiometric to the amount of GSH thiolate formed in the G-site. The apparent  $pK_a$  value for the bound GSH, calculated with this potentiometric approach, is  $6.18 \pm 0.09$ ; very similar values are found by spectrophotometric ( $6.20 \pm 0.12$ ) and by kinetic ( $6.00 \pm 0.08$ ) experiments. Binding of *S*-hexylglutathione does not cause any proton release. Stopped-flow data obtained by means of an acid–base indicator show that the proton extrusion process (apparent  $t_{1/2} = 1.1 \pm 0.1$  ms at 15 °C) is not rate limiting in turnover (apparent  $t_{1/2} = 34 \pm 4$  ms at 15 °C). By comparing the kinetic behavior of three distinct events occurring during the binding of GSH to the enzyme, i.e., proton release, ionization of bound GSH and quenching of intrinsic fluorescence, it appears that the binding process follows a multistep mechanism possibly involving the conformational transition of a weak precomplex into the final Michaelis complex. This step is modulated by helix 2 motions and may be rate limiting at physiological GSH concentrations. These findings, coming from kinetic studies, are consistent with NMR data [Nicotra, M., Paci, M., Sette, M., Oakley, A. J., Parker, M. W., Lo Bello, M., Caccuri, A. M., Federici, G., and Ricci, G. (1998) *Biochemistry* 37, 3020–3027] and time-resolved fluorescence experiments [Stella, L., Caccuri, A. M., Rosato, N., Nicotra, M., Lo Bello, M., De Matteis, F., Mazzetti, A. P., Federici, G., and Ricci, G., manuscript in preparation].

Cytosolic glutathione transferases (GSTs,<sup>1</sup> EC 2.5.1.18) are a family of detoxifying enzymes able to conjugate GSH to a variety of organic compounds which contain an electrophilic center (1). The GSTs are presently grouped into five classes: Alpha, Mu, Pi, Theta and Sigma (2–5). A critical step in catalysis is the ionization of the sulfhydryl group of GSH, as its undissociated form is about  $10^9$  times less reactive toward electrophiles (6). In fact, a common feature of all GSTs, which also have very similar GSH binding sites (G-sites), is to lower the apparent  $pK_a$  of the bound GSH from 9.1 to about 6.0–6.6. Evidence for this ability comes from the direct spectrophotometric observation of  $GS^-$  in the active site of the Mu class GSTs M3-3 (7) and M4-4 (8) at neutral pH values, as well as from indirect

kinetic evidence for the Alpha and Pi class GSTs (9, 10). The origin of this deprotonating property is unclear, as no evident positive electrostatic field is found near the bound GSH. The hydroxyl group of a conserved tyrosine (for instance, Tyr 6 in the Mu class GST M3-3, Tyr 7 in the Pi class GST P1-1 and Tyr 9 in the Alpha class GST A1-1), which H-bonds to the sulfur atom of GSH, probably stabilizes and orientates the thiolate in a productive fashion (6), but its role as an efficient thiol proton acceptor in catalysis is controversial due to its  $pK_a > 8.0$  (9, 11, 12). Therefore, some questions are still open; in particular, does a true basic residue exist in the G-site and is it able to act as thiol proton acceptor? Furthermore, when and how does this proton leave the G-site during turnover? Recently, it has been suggested that the Glu-carboxylate of GSH itself could act as proton acceptor by raising its normal  $pK_a$  upon binding to the enzyme; in that case, the proton could leave the active site when the product is released (13). The involvement of a water molecule in a proton shuttle has also been invoked since thiol and carboxylate groups of GSH are about 7 Å apart in the G-site (13). On the basis of recent observations that local flexibility of the protein structure near the G-site in GST P1-1 has a role in catalysis (14, 15), a theoretical study proposes that protein motions may facilitate the proton transfer from the thiol to the Glu-carboxylate group (16).

<sup>†</sup> This work was partially supported by a grant of Ministero dell'Università e della Ricerca Scientifica e Tecnologica (funds 40% and 60%) and by a grant from Consiglio Nazionale delle Ricerche, Progetto Finalizzato ACRO.

\* Address for correspondence: Department of Biology, University of Rome, "Tor Vergata", Viale della Ricerca Scientifica, 00133 Rome, Italy. Tel: +39-6-72594375. Fax: +39-6-2025450. E-mail: ricci@utovrm.it.

<sup>‡</sup> University of Rome "Tor Vergata".

<sup>§</sup> University of Rome "La Sapienza".

<sup>||</sup> Children's Hospital IRCCS of Rome.

<sup>1</sup> Abbreviations: CDNB, 1-chloro-2,4-dinitrobenzene; GST, glutathione transferase.

In this complex scenario our goal has been to define unambiguously the fate of this thiol proton. By means of potentiometric measurements, we demonstrate here that when the GSH-GST P1-1 complex is formed, the thiol proton is not neutralized by any basic residue in the G-site, but leaves the active site, quantitatively. Stopped-flow data suggest that the proton extrusion process cannot be rate limiting in turnover. Pre-steady-state kinetic studies also indicate that binding follows a multistep mechanism, in which a conformational change of the binary complex is likely to be rate determining at physiological GSH concentrations.

## EXPERIMENTAL PROCEDURES

**Materials.** Human placenta GST P1-1 was expressed in *Escherichia coli* and purified as previously described (17). Removal of phosphate buffer from protein solutions was obtained by a G-25 Sephadex column (2 × 50 cm), equilibrated with 0.1 M NaCl. All solutions used contained 0.1 mM ethylenediaminetetracetic acid. GSH and *S*-hexylglutathione were Sigma products.

**Spectroscopic Evidence for GSH Ionization.** Difference spectra of GS<sup>−</sup> bound to GST P1-1 were obtained with a double-beam Uvicon 940 Kontron spectrophotometer equipped with a thermostated cuvette compartment. Spectra were recorded in the range 230–310 nm at 25 °C. In a typical experiment 1 mM GSH was added to GST P1-1 (13 μM active sites) in 1 mL of 0.01 M potassium phosphate buffer, pH 6.70. From the resulting spectrum, the contributions from free GSH and free enzyme were subtracted. The difference spectra at pH < 6.0 were obtained using 0.01 M sodium acetate buffers. Quantitation of the thiolate was made assuming an  $\epsilon_{239\text{nm}}$  of 5500 M<sup>−1</sup>cm<sup>−1</sup> (6). The amount of the total GSH bound to the enzyme, [GSH + GS<sup>−</sup>]<sub>b</sub> at different pH values and in the presence of 1 mM GSH, was determined on the basis of the affinity of the enzyme for GSH calculated at each pH by fluorometric experiments (18).

**Kinetic Experiments.** Steady-state kinetics of GST P1-1 activity with 1-chloro-2,4-dinitrobenzene (CDNB) as cosubstrate was measured at 340 nm, where the product absorbs ( $\epsilon_{340\text{nm}}$  = 9600 M<sup>−1</sup>cm<sup>−1</sup>). Kinetic parameters were determined under steady-state conditions as previously described (14, 15).

**Detection of Thiol Proton Extrusion.** Potentiometric measurements of thiol proton extrusion were done at 25 °C with a Corning 140 pH meter equipped with an Ingold U402-S7/120 pH electrode. In a typical experiment, made under N<sub>2</sub> atmosphere to minimize possible CO<sub>2</sub> interference, a GSH solution (0.1 M in 0.1 M NaCl) was titrated to pH 7.43 with 0.1 N NaOH. Of this solution, 0.02 mL was then added to 2 mL of GST P1-1 (77 μM active sites in 0.1 M NaCl) at exactly the same pH value. pH changes were recorded within 2 min after mixing. Quantitation of the released thiol proton was made by suitable additions of 10 or 1 mM NaOH solutions to reach the initial pH value. All pH adjustments were made by using NaOH solutions prepared from a commercial Standard 0.1 M NaOH solution (Fluka) containing less than 0.01% sodium carbonate.

**Stopped-Flow Analysis.** Stopped-flow measurements were made on an Applied Photophysics kinetics spectrometer stopped-flow instrument, equipped with a thermostated 1 cm light path observation chamber. Dead-time of the instrument

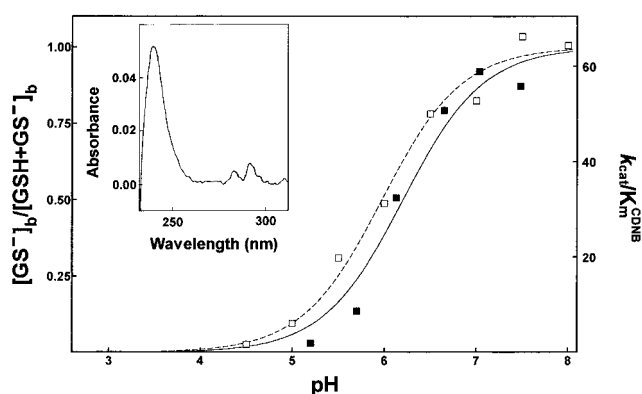


FIGURE 1: Spectroscopic and kinetic evidence for GSH ionization. Spectra of GS<sup>−</sup> in the binary complex GSH-GST P1-1 (1 mM GSH, 13 μM GST P1-1 under different pH conditions) were obtained as described in the Experimental Procedures. The concentration of the thiolate bound to the G-site [GS<sup>−</sup>]<sub>b</sub> was calculated by assuming an  $\epsilon_{239\text{nm}}$  of 5500 M<sup>−1</sup>cm<sup>−1</sup>. The concentration of total bound glutathione [GSH + GS<sup>−</sup>]<sub>b</sub> was calculated on the basis of fluorometric experiments (15) performed at each pH value. (■) pH dependence of [GS<sup>−</sup>]<sub>b</sub>/[GSH + GS<sup>−</sup>]<sub>b</sub>; (□) pH dependence of  $k_{\text{cat}}/K_m^{\text{CDNB}}$ . Data shown in the figure represent the mean of three different experiments; the standard error for each point does not exceeds 7%. Lines are least-squares fits of the experimental data by the equation  $Y = Y_{\text{lim}}/(1 + 10^{-\text{pH}/K_a})$ , where  $Y$  represents [GS<sup>−</sup>]<sub>b</sub>/[GSH + GS<sup>−</sup>]<sub>b</sub> (full line) or  $k_{\text{cat}}/K_m^{\text{CDNB}}$  (dashed line). (Inset) Spectrum of GS<sup>−</sup> bound to GST P1-1 at pH 6.70.

was 1 ms as determined by independent experiments employing reduced horse myoglobin and carbon monoxide. The flux time was 2 ms after triggering. Kinetics of the thiol proton extrusion was studied by rapid mixing of GST P1-1 [88 μM active sites in 0.1 M NaCl and 10 μM bromocresol purple indicator (Fluka), pH 6.5] with an identical volume of GSH or *S*-hexylglutathione (from 0.1 mM up to 6 mM in 0.1 M NaCl and 10 μM bromocresol purple, pH 6.5). The initial absorbance of the resulting solution at 588 nm (where the deprotonated indicator absorbs) was approximately 0.38. No interactions have been found between GST P1-1 and this acid–base indicator; for example, no changes in enzymatic activity were observed at the concentration applied. Kinetics of the GSH thiolate formation was followed at 240 nm by rapid mixing of GST P1-1 (88 μM active sites in 0.1 M NaCl, pH 6.5) with an identical volume of GSH (from 0.1 mM up to 6 mM in 0.1 M NaCl, pH 6.5). The kinetics of GSH binding to GST P1-1 was studied by following the quenching of the intrinsic fluorescence at 340 nm ( $\lambda_{\text{ex}}$  = 295 nm) after rapid mixing of GST P1-1 (88 μM active sites in 0.1 M NaCl, pH 6.5) with an identical volume of GSH (from 0.1 mM up to 6 mM in 0.1 M NaCl, pH 6.5). The apparent first-order rate constant for the release of GSH from the binary complex GSH-GST P1-1 was determined by rapid mixing of a solution of the binary complex [GST P1-1, 88 μM active sites in 0.1 M NaCl, pH 6.5, in the presence of a nonsaturating GSH concentration (0.1 mM)], with an identical volume of 0.1 M NaCl, pH 6.5. The release of GSH upon dilution was monitored by following the increase of the protein intrinsic fluorescence at 340 nm ( $\lambda_{\text{ex}}$  = 295 nm).

**Kinetic Data Analysis.** Apparent first-order rate constants ( $k_{\text{obs}}$ ) were calculated from the experimental traces of protein fluorescence quenching and absorbance changes at 240 and 588 nm, obtained after mixing the enzyme with different

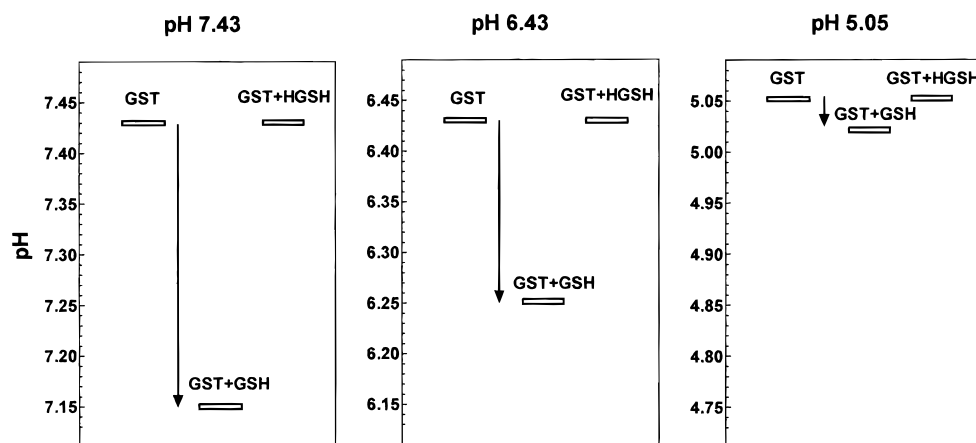


FIGURE 2: Potentiometric evidence for the thiol proton extrusion. Panels show pH measurements observed after mixing 0.02 mL of 0.1 M GSH or 0.1 M S-hexylglutathione (HGSH) with 2 mL of 77  $\mu$ M GST P1-1, all solutions containing 0.1 M NaCl and titrated to the same pH value. The initial pH values are 7.43, 6.43, and 5.05.

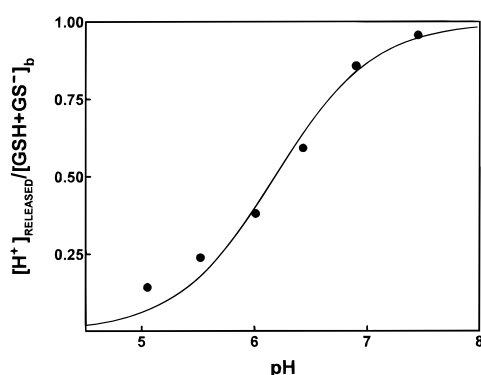


FIGURE 3: pH dependence of the thiol proton release. The concentration of the released thiol proton ( $[H^+]_{\text{released}}$ ) was calculated at each pH as described in the Experimental Procedures and normalized to the total bound glutathione ( $[GSH + GS^-]_b$ ). Data shown in the figure represent the mean of three different experiments; the standard error for each point does not exceed 5%. Solid line represents the computer fit of the experimental data to the equation reported in the legend of Figure 1. The pH dependence of the  $GS^-$  formation (solid line, Figure 1) is exactly coincident with the pH dependence of the thiol proton release reported in this figure.

GSH concentrations (see legend of Figure 5 for details), using the program MATLAB (Mathworks, Natick, MA). The same experimental data were fitted to Scheme 1 to obtain the microscopic rate constants listed in Table 2 using the program FACSIMILE (Atomic Energy Authority, Harwell, Didcot, Oxon, U.K.) running on an Intel Pentium based personal computer. The program carries out the simultaneous fitting of the observed time courses into Scheme 1 by means of numerical integration of the ordinary differential equations. By using numerical integration we also obtained simulated time dependences of the observed events (fluorescence quenching, absorbance changes at 240 nm and at 588 nm). From these simulated traces we calculated the apparent first-order rate constants plotted as the continuous line in Figure 5. The protein fluorescence quenching was attributed to the appearance of  $E^*-GSH$ ,  $H^+-E^*-GS^-$  and  $E^*GS^-$  species; the absorbance change at 240 nm was attributed to the appearance of  $H^+-E^*-GS^-$  and  $E^*GS^-$  species, whereas the absorbance change at 588 nm was attributed to the appearance of the  $E^*GS^-$  species (see Scheme 1).

## RESULTS

**Spectroscopic Evidence for GSH Ionization in the G-Site.** Direct evidence for the ionization of the enzyme-bound GSH comes from UV difference spectroscopy. Similarly to that observed with the rat liver GSTs M3-3 (7) and M4-4 (8), the spectrum of a solution containing GST P1-1 (13  $\mu$ M) and GSH (1 mM) at pH 6.70, after subtracting the contributions of free GST and free GSH, shows an absorption band centered at 239 nm (Figure 1, inset), which is typical of the mercaptide ion (6). By assuming a  $\epsilon_{239\text{nm}}$  of 5500  $M^{-1} \text{cm}^{-1}$  for the ionized GSH (6), it can be calculated that 9.3  $\mu$ M  $GS^-$  is formed at the active site. The pH dependence of the bound thiolate gives an apparent  $pK_a$  of  $6.20 \pm 0.12$  (Figure 1). This spectroscopic evidence agrees well with kinetic data; the pH dependence of  $k_{\text{cat}}/K_m^{\text{CDNB}}$ , which should reflect the ionization of the bound GSH in the GST-GSH binary complex (8), shows an apparent  $pK_a$  of  $6.00 \pm 0.08$  (Figure 1).

**Proton Release after GSH Binding.** Direct evidence for the release of the thiol proton upon GSH binding is obtained by mixing unbuffered GST P1-1 and GSH solutions (both in 0.1 M NaCl), titrated to the same initial pH value. The proton release is monitored by potentiometric measurements. For a correct interpretation of these experiments, the substrate binding affinity and kinetic parameters of GST P1-1 in 0.1 M NaCl must be compared to those observed in 0.1 M phosphate buffer. No differences have been found for  $K_m^{\text{GSH}}$  and for the pH dependence of  $k_{\text{cat}}/K_m^{\text{GSH}}$ , while a 50% decrease both of  $k_{\text{cat}}$  and  $K_m^{\text{CDNB}}$  values have been observed in the absence of any buffer, between pH 5.0 and 8.0 (data not shown). The unchanged  $k_{\text{cat}}/K_m^{\text{CDNB}}$  ratio suggests the lowering of these kinetic parameters may be due to a partial nonproductive binding of the cosubstrate in the absence of phosphate ions. In any case, the affinity for GSH and its  $pK_a$  in the G-site are unaffected by the lack of phosphate buffer. Figure 2 shows potentiometric data from three representative experiments made at pH 7.43, 6.43, and 5.05, where about 90, 65, and 10% of the bound glutathione is deprotonated, respectively. By mixing 1 mM GSH with 77  $\mu$ M GST P1-1, we observe a pH decrease ranging between 0.28 (at pH 7.43) and 0.03 units (at pH 5.05). No pH changes occur when GSH or GST P1-1 solutions are diluted separately. Clearly, these potentiometric data cannot be used

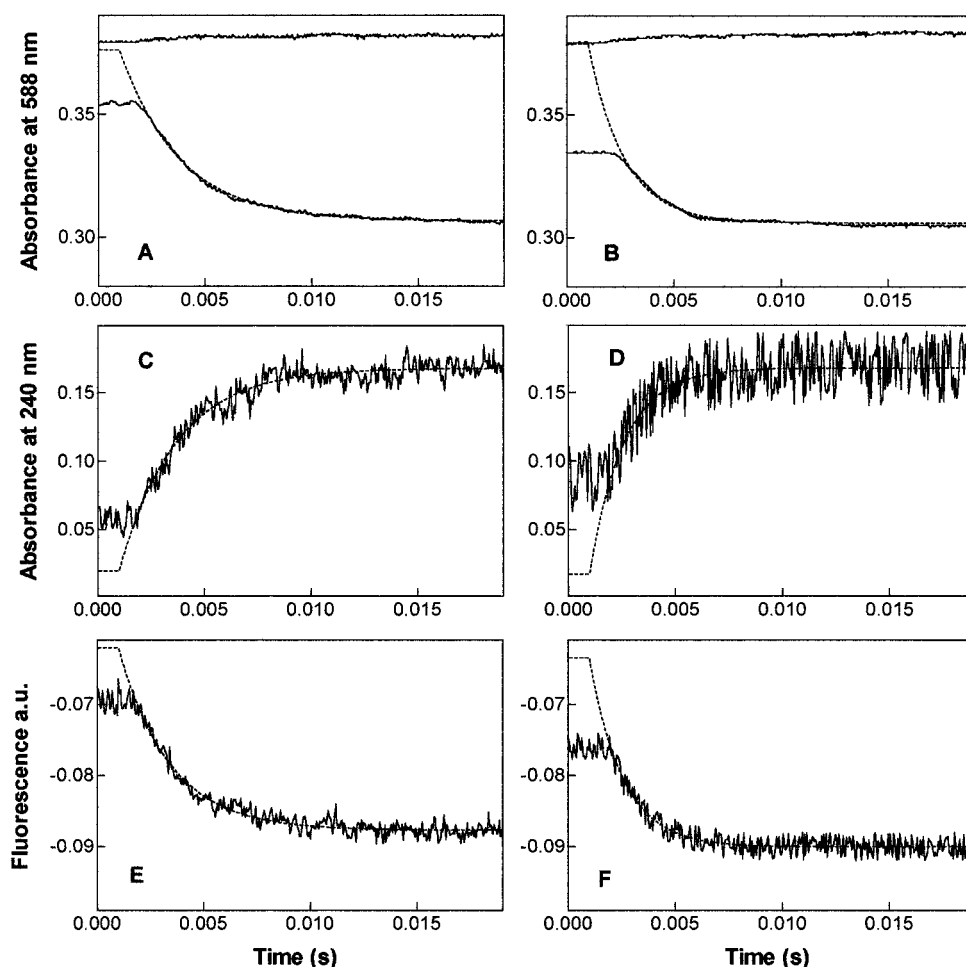


FIGURE 4: Stopped-flow experiments. (A and B) Kinetics of thiol proton release. Stopped-flow experiments were performed by rapid mixing GST P1-1 solution (88  $\mu$ M active site in 0.1 M NaCl and 10  $\mu$ M bromocresol purple, pH 6.5) with an identical volume of a *S*-hexylglutathione solution (2 mM in 0.1 M NaCl and 10  $\mu$ M bromocresol purple, pH 6.5) (upper trace) or of a GSH solution (2 mM in 0.1 M NaCl and 10  $\mu$ M bromocresol purple, pH 6.5) (lower trace). Temperature was 5  $^{\circ}$ C (A) and 15  $^{\circ}$ C (B). The reaction was followed at 588 nm. (C and D) Kinetics of ionization of the bound GSH. Stopped-flow experiments were performed by rapid mixing GST P1-1 solution (88  $\mu$ M active site in 0.1 M NaCl, pH 6.5) with an identical volume of a GSH solution (2 mM in 0.1 M NaCl pH 6.5). The reaction was followed at 240 nm. Temperature was 5  $^{\circ}$ C (C) and 15  $^{\circ}$ C (D). (E and F) Kinetics of quenching of the protein intrinsic fluorescence. Stopped-flow experiments were performed by rapid mixing a GST P1-1 solution (88  $\mu$ M active site in 0.1 M NaCl, pH 6.5) with an identical volume of a GSH solution (2 mM in 0.1 M NaCl pH 6.5). The reaction was followed at 340 nm by exciting at 295 nm; temperature was 5  $^{\circ}$ C (E) and 15  $^{\circ}$ C (F). The mean of six different experiments is reported in each panel. The instrument dead time was 1 ms with a flux time of 2 ms after mixing. Dotted line represents a least-squares fit of the experimental data by a simple exponential.

as such to titrate the released protons, owing to the possible buffering action of the protein. A convenient quantitation is achieved by suitable additions of NaOH to the final GST-GSH mixture to regain the initial pH value. By this back-titration, the released thiol proton is found 64, 41, and 8  $\mu$ M at pH 7.43, 6.43, and 5.05, respectively. The curve fit for the pH dependence of the proton release (Figure 3,  $pK_a = 6.18 \pm 0.09$ ) is exactly coincident with that for the pH dependence of thiolate formation (Figure 1,  $pK_a = 6.20 \pm 0.12$ ). Therefore, the amount of protons released (between pH 5.05 and 7.43) is stoichiometric to the amount of thiolate formed in the G-site. Upon replacing GSH with *S*-hexylglutathione, a GSH analogue, which binds to the active site with high affinity ( $K_D = 20 \mu$ M; 19), no pH changes are observed (Figure 2). This suggests that the released proton comes exclusively from the sulfhydryl ionization and that no other relevant  $pK_a$  changes occur in the protein and in the GSH molecule.

**Kinetics of Proton Extrusion.** The use of a stopped-flow apparatus and a suitable acid-base indicator such as bro-

mocresol purple ( $pK_a = 6.30$ ) allowed us to determine the proton extrusion kinetics; these experiments were performed at 15 and 5  $^{\circ}$ C in the absence of any inorganic buffer, by rapidly mixing GST and GSH. As shown in Figure 4, the proton release yields an absorbance decrease of about 0.08 at 588 nm and this process ends within 6 ms. No absorbance changes occur when *S*-hexylglutathione is mixed with GST P1-1 (Figure 4). By fitting these kinetic data to a single-exponential decay, an apparent  $t_{1/2} = 1.1 \pm 0.1$  ms is calculated at 15  $^{\circ}$ C which increases to  $1.9 \pm 0.2$  ms at 5  $^{\circ}$ C (see Figure 4 and Table 1). These results rule out the possibility that the thiol proton extrusion represents the rate-limiting step in catalysis; in that case, a much longer  $t_{1/2}$  (34 ms) is expected on the basis of a measured  $k_{cat}$  of 20  $s^{-1}$  at 15  $^{\circ}$ C. The possibility that this process is much faster but rate limited by a previous step has been checked by following two distinct events which occur during the interaction of GSH with the enzyme, i.e., ionization of the GSH sulfhydryl group and quenching of the protein intrinsic fluorescence.

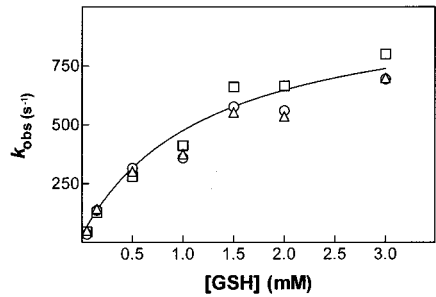


FIGURE 5: Dependence of the observed first-order rate constants versus [GSH]. Apparent first-order kinetic constants for proton extrusion (○), GSH ionization (△) and protein fluorescence quenching (□) were obtained with the same experimental procedure described in the legend of Figure 4 at different GSH concentrations (from 0.05 to 3 mM, after mixing) and at 5 °C. Although pseudo-first-order conditions are not strictly observed for the experiments at the two lowest GSH concentrations, the experimental traces were quite well described by a single-exponential decay. The continuous line represents the apparent first-order rate constants obtained from the simulation of the observed time courses into Scheme 1 by using numerical integration of the ordinary differential equation and by employing the microscopic rate constants listed in Table 2.

Scheme 1

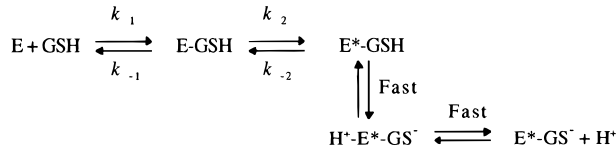


Table 1: Pre-Steady-State Kinetic Parameters Derived by Stopped-Flow Experiments<sup>a</sup>

	$k_{\text{obs}}$ (s <sup>-1</sup> ) (5 °C)	$k_{\text{obs}}$ (s <sup>-1</sup> )(15 °C)
proton extrusion	357 ± 30 (1.9 ms)	600 ± 50 (1.1 ms)
GSH thiolate formation	375 ± 15 (1.8 ms)	632 ± 30 (1.1 ms)
fluorescence quenching	412 ± 25 (1.7 ms)	643 ± 45 (1.1 ms)

<sup>a</sup> Apparent rate constants were calculated from the stopped-flow experiments reported in Figure 4.  $t_{1/2}$  values are reported in parentheses.

Table 2: Microscopic Constants<sup>a</sup> of the GSH Binding Process at 5 °C

$k_1$	$\geq 10^6 \text{ M}^{-1} \text{ s}^{-1}$
$k_{-1}$	$\geq 1250 \text{ s}^{-1}$
$k_{-1}/k_1$	1.25 mM
$k_2$	$1000 \pm 50 \text{ s}^{-1}$
$k_{-2}$	$30 \pm 6 \text{ s}^{-1}$
$k_{-2}^b$	$37 \pm 5 \text{ s}^{-1}$
$k_{-2}/k_2$	0.037

<sup>a</sup> All microscopic rate constants must be referred to Scheme 1 and are calculated by fitting the stopped-flow data as described in the Experimental Procedures. <sup>b</sup> Calculated by the dilution experiment reported in the text.

**Kinetics of Thiolate Formation.** The sulfhydryl ionization of bound GSH is studied by means of a set of pre-steady-state spectrophotometric measurements at 240 nm where the thiolate absorbs (6). Also, these experiments were performed in the absence of any inorganic buffer, by mixing GST and GSH. Figure 4 shows experimental traces obtained at 5 and 15 °C. Kinetic data can be fitted to a single-exponential equation, and  $t_{1/2}$  values calculated at 5 and 15 °C are close to those found for the proton release at the same temperature (Table 1). Thus, these events are synchronous on the millisecond time scale.

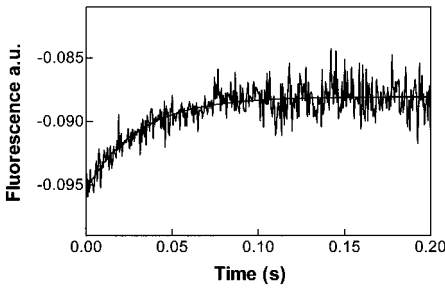


FIGURE 6: Kinetics of GSH release from the binary complex. Stopped flow experiments were performed by rapid mixing GST P1-1 (88 μM active site in 0.1 M NaCl, pH 6.5) in the presence of nonsaturating GSH (0.1 mM) with an identical volume of 0.1 M NaCl, pH 6.5. The release of GSH from the enzyme was monitored by following the increase of fluorescence at 340 nm ( $\lambda_{\text{ex}} = 295 \text{ nm}$ ). Temperature was 5 °C. Dotted line represents a least-squares fit of the experimental data by a simple exponential. The mean of six different experiments is reported in the figure.

**Kinetics of the Protein Fluorescence Quenching.** Quenching of the enzyme fluorescence due to the interaction of the substrate with the G-site possibly reflects the first event of the binding process; this spectroscopic perturbation is almost independent of the ionization of GSH (18) and may be used, under equilibrium conditions, to calculate the thermodynamic dissociation constant of the binary GSH–GST P1-1 complex at pH 6.5. At 5 °C,  $K_D$  is  $55 \pm 10 \mu\text{M}$ , while at 15 °C, it is  $50 \pm 12 \mu\text{M}$ .

Pre-steady-state fluorometric experiments, performed as described in Experimental Procedures, indicate that the quenching event is synchronous with thiolate formation and with proton extrusion, showing apparent  $t_{1/2} = 1.1 \pm 0.1 \text{ ms}$  at 15 °C and  $1.7 \pm 0.1 \text{ ms}$  at 5 °C (Table 1).

The dependence on GSH concentration of the apparent first-order rate constant for the fluorescence quenching is not linear, but follows an hyperbolic behavior (Figure 5), which reaches a limiting value of  $1000 \pm 50 \text{ s}^{-1}$  at GSH concentrations higher than 5 mM. The data in Figure 5 were collected only at 5 °C, since at 15 °C the reaction of the enzyme with GSH at concentrations higher than 1 mM is too fast to be analyzed correctly. Apparent kinetic constants for thiolate formation as well as for proton extrusion also follow a very similar hyperbolic dependence (Figure 5). This peculiar kinetic behavior suggests an interpretation in terms of a multistep binding mechanism, which will be discussed below.

**GSH Release from the GSH–GST Complex.** Kinetics of GSH release from the binary complex was studied by rapid dilution of a solution of GST P1-1 in equilibrium with nonsaturating levels of GSH. The increase of fluorescence at 340 nm visualizes the release of GSH upon dilution (Figure 6). Under these conditions, the first-order rate constant is  $37 \pm 5 \text{ s}^{-1}$  at 5 °C (Table 2).

# DISCUSSION

The fate of the thiol proton coming from the ionization of GSH bound to GST P1-1 has been studied. Spectroscopic and kinetic data confirm that the sulfhydryl group of the bound GSH undergoes a forced deprotonation showing an apparent  $pK_a$  of 6.00–6.20 (see Figure 1), close to that found for other GSTs ( $pK_a = 6.0$ –6.6). Potentiometric experiments clearly prove that the proton coming from the bound GSH

is released quantitatively into the surrounding solution (see Figures 2 and 3). This process does not require the presence of any cosubstrate, and it is not related to the formation or release of a product since it occurs in the absence of any enzyme turnover. Moreover, stopped-flow measurements (see Figure 4 and Table 1) indicate that proton release has an apparent  $t_{1/2} = 1.1 \pm 0.1$  ms at 15 °C and therefore cannot be rate limiting in catalysis.

The above findings may help to understand the proposed roles of Tyr 7 and of Glu-carboxylate of GSH in the deprotonation of the substrate (11, 13). The release of the thiol proton, stoichiometric to the  $\text{GS}^-$  formed in the active site, makes it unlikely that either protein or substrate acts quantitatively as the thiol proton acceptor. Assuming that the presence of the cosubstrate does not alter the fate of this proton, it also seems improbable that, during turnover, the thiol proton leaves the active site only when the enzymatic product is released (13). Clearly, both Tyr 7 and the Glu-carboxylate might still have a role in GSH ionization, but only as transient proton carriers. This function may require a small amount of tyrosinate or carboxylate as proton acceptors, and such a possibility is less irreconcilable with the  $\text{pK}_a$  values found for these residues. However, the thermodynamic driving force of the proton extrusion process cannot be clarified by the present investigation.

In a second experimental series, we attempted to dissect the GSH binding process by comparing the kinetic behavior of three distinct events occurring during the interaction of GSH with the G-site, i.e., quenching of intrinsic fluorescence of the enzyme, thiolate formation, and proton extrusion. Apparently, all these events show very similar kinetics (see Table 1). This could mean that an initial step is rate limiting while all following are faster. This possibility is likely, given the observation that at low GSH concentrations all rate constants depend on [GSH], while only the first event, i.e., the protein fluorescence quenching, should reflect a bimolecular reaction (see Figure 5). Furthermore, all the kinetic constants show a hyperbolic dependence on GSH. All these findings are diagnostic for a two-step binding mechanism (20). A reasonable (but not unequivocal) scheme which agrees with experimental data is presented in Scheme 1.

This proposed minimal mechanism involves a structural transition of an unquenched precomplex E–GSH to give the quenched Michaelis complex  $\text{E}^*\text{--GSH}$ . This step becomes rate limiting at physiological GSH concentrations (5–10 mM), while GSH ionization and proton output follow and are very fast events. The possibility that thiolate formation may precede and thus cause the quenching event is less plausible. In fact, fluorescence quenching does not depend on GSH deprotonation as the enzyme is also quenched by *S*-methylglutathione (18). An alternative two-step binding mechanism is also possible but requires at least two slow interconverting apo-GST conformers in which binding of GSH occurs only in one conformer. This possibility is unlikely as, in that case, the kinetic rate constants should decrease by increasing [GSH] (20).

Nonlinear fitting of all experimental data to Scheme 1 gives an estimation of some microscopic rate constants (Table 2). The minimum value of the second-order rate constant for the GSH binding ( $k_1$  in Scheme 1) is  $10^6 \text{ M}^{-1} \text{ s}^{-1}$ , which also represents the angular coefficient of the

tangent to the hyperbolic dependence of  $k_{\text{obs}}$  on [GSH] (see Figure 5) at the lowest GSH concentration (20). The first-order rate constant for the structural transition of the unquenched binary complex E–GSH toward the quenched  $\text{E}^*\text{--GSH}$  complex ( $k_2$  in Scheme 1) is  $1,000 \text{ s}^{-1}$ , representing the asymptotic value of  $k_{\text{obs}}$  versus [GSH] (Figure 5) at the highest GSH concentration (20). The dissociation rate constant  $k_{-2}$  is  $37 \text{ s}^{-1}$  as calculated by a direct dilution experiment (see Figure 6) and confirmed by the fitting procedure ( $30 \text{ s}^{-1}$ ). From the fitting procedure, the rate constant for the dissociation of the E–GSH complex ( $k_{-1}$ ) has been found related to  $k_1$  so that  $k_{-1}/k_1 = 1.25 \text{ mM}$ , in very good agreement with the ratio  $k_{-1}/k_1$  calculated according to a two-step binding mechanism as reported by Fersht (20). This ratio represents the dissociation constant  $K_{\text{D1}}$  of the precomplex to give free GSH and free enzyme. It follows that the minimal value for  $k_{-1}$  is  $1250 \text{ s}^{-1}$ . From the fitting procedure, it also results that the experimental data are well described by any  $k_1$  value  $\geq 10^6 \text{ M}^{-1} \text{ s}^{-1}$  and proportional  $k_{-1}$  values  $\geq 1250 \text{ s}^{-1}$ . A precise value of the rate constant for the ionization step cannot be estimated but the experimental data are well described by any value  $\geq 5000 \text{ s}^{-1}$ .

On the basis of the above values for the microscopic rate constants, the equilibrium constant for the binary complex  $\text{E}^*\text{--GSH}$  to give E–GSH can be calculated as  $K_{\text{eq}} = k_{-2}/k_2 = 0.037$ . The overall apparent dissociation constant for the complex  $\text{E}^*\text{--GSH}$  to give free GSH and free GST P1-1 is then  $K_{\text{D}} = K_{\text{D1}}K_{\text{eq}} = 46 \text{ }\mu\text{M}$ . This value is close to that experimentally found at 5 °C by steady-state fluorometric experiments ( $55 \pm 10 \text{ }\mu\text{M}^{-1}$ ).

We report here, for the first time, evidence for the existence of a precomplex (E–GSH) in the enzymatic mechanism of GSTs. In this early interaction, GSH binds to the enzyme less tightly with respect to the more stable Michaelis complex ( $\text{E}^*\text{--GSH}$ ), thus suggesting that GSH in the precomplex has not yet established some important interactions with protein residues. More precisely, by comparing  $K_{\text{D1}}$  and  $K_{\text{eq}}$ , it results that the tightly bound complex is about 7.6 kJ/mol more stabilized than the precomplex. Interestingly, comparison of the GSH conformation in the GST–GSH crystal complex with that in the early stage of the binding process (as shown by NMR data) indicates that the glutamyl moiety of GSH interacts differently with protein residues (21).

It is also interesting to discuss the possible role of helix 2 in the GSH binding step. This irregular helix displays the highest flexibility of Domain 1 (22). Recently, it has been found that diffusion-controlled motions of helix 2 also modulate the affinity of the enzyme toward GSH (14). Now, on the basis of the present data, a possible correlation between all these observations can be made: this mobile loop, via Trp 38 and Lys 44 that both interact with the glycyl end of the bound GSH, could act as a flexible GSH carrier which through its motions drives the substrate to find a correct anchorage for its glutamyl moiety in the G-site. Only in this final situation is Trp 38 quenched, probably due to a more rigid conformation. This scenario is reasonable in the light of dynamic fluorescence data showing that Trp 38 mainly exists in a quite rigid environment in the GSH–GST P1-1 complex. However, a significant fraction of the binary complex, which may represent the weakly bound precomplex, is formed by multiple interconverting conformers

showing high flexibility of helix 2 (Stella et al., manuscript in preparation). The proposed functional role of helix 2 motions is consistent with the dramatic loss of affinity toward GSH after replacement of either Trp 38 (23) or Cys 47, which resides at the end of helix 2 and is important for the correct fluctuations of this loop (24, 14).

Evidence that structural transitions of this enzyme, involving specific regions of the polypeptide chain, are rate determining in the catalytic mechanism of GST P1-1 (14, 15) as well as in the binding mechanism of the substrate (this paper) clearly indicates that some of the major remaining questions concerning this enzyme could be solved by molecular dynamics studies. Such studies are currently pursued in our laboratory.

## REFERENCES

1. Habig, W. H., & Jakoby, W. B. (1981) *Methods Enzymol.* 77, 398–405.
2. Mannervik, B., Alin, P., Guthenberg, C., Jennson, H., Tahir, M. K., & Jornvall, H. (1985) *Proc. Natl. Sci. U.S.A.* 82, 7202–7206.
3. Meyer, D. J., Coles, B., Pemble, S. E., Gilmore, K. S., Fraser, G. M., & Ketterer, B. (1991) *Biochem. J.* 274, 404–414.
4. Buetler, T. M., & Eaton, D. L. (1992) *Environ. Carcinog. Ecotoxicol. Rev.* 10, 181–203.
5. Meyer, D. J., & Thomas, M. (1995) *Biochem. J.* 311, 739–742.
6. Armstrong, R. N. (1991) *Chem. Res. Toxicol.* 4, 131–139.
7. Liu, S., Zhang, P., Ji, X., Johnson, W. W., Gilliland, G. L., & Armstrong, R. N. (1992) *J. Biol. Chem.* 267, 4296–4299.
8. Graminski, G. F., Kubo, Y., & Armstrong, R. N. (1989) *Biochemistry* 28, 3562–3568.
9. Björnstedt, R., Stenberg, G., Widersten, M., Board, P. G., Sinning, I., Jones, T. A., & Mannervik, B. (1995) *J. Mol. Biol.* 247, 765–773.
10. Kong, K. H., Takasu, K., Inoue, H., & Takahashi, K. (1992) *Biochem. Biophys. Res. Commun.* 184, 194–197.
11. Atkins, W. M., Wang, R. W., Bird, A. W., Newton, D. J., & Lu, A. Y. H. (1993) *J. Biol. Chem.* 268, 19188–19191.
12. Kolm, R. H., Sroga, G. E., & Mannervik, B. (1992) *Biochem. J.* 285, 537–540.
13. Widersten, M., Björnstedt, R., & Mannervik, B. (1996) *Biochemistry* 35, 7731–7742.
14. Ricci, G., Caccuri, A. M., Lo Bello, M., Rosato, N., Mei, G., Nicotra, M., Chiessi, E., Mazzetti, P., & Federici, G. (1996) *J. Biol. Chem.* 271, 16187–16192.
15. Caccuri, A. M., Ascenzi, P., Antonini, G., Parker, M. W., Oakley, A. J., Chiessi, E., Nuccetelli, M., Battistoni, A., Bellizia, A., & Ricci, G. (1996) *J. Biol. Chem.* 271, 16193–16198.
16. Zheng, Y. J., & Ornstein, R. L. (1996) *J. Biomol. Struct. Dyn.* 14, 231–233.
17. Lo Bello, M., Battistoni, A., Mazzetti, A. P., Board, P. G., Muramatsu, M., Federici, G., & Ricci, G. (1995) *J. Biol. Chem.* 270, 1249–1253.
18. Caccuri, A. M., Aceto, A., Rosato, N., Di Ilio, C., Piemonte, F., & Federici, G. (1991) *It. J. Biochem.* 40, 304–311.
19. Mannervik, B. (1985) *Adv. Enzymol. Relat. Areas Mol. Biol.* 57, 357–417.
20. Fersht, A. (1985) *Enzyme structure and mechanism*, 2nd ed., pp 121–154, Freeman, W. H., & Company, NY.
21. Nicotra, M., Paci, M., Sette, M., Oakley, A. J., Parker, M. W., Lo Bello, M., Caccuri, A. M., Federici, G., & Ricci, G. (1998) *Biochemistry* 37, 3020–3027.
22. Lo Bello, M., Pastore, A., Petruzzelli, R., Parker, M. W., Wilce, M. C. J., Federici, G., & Ricci, G. (1993) *Biochem. Biophys. Res. Commun.* 194, 804–810.
23. Nishihira, J., Ishibashi, T., Sakai, M., Nishi, S., & Kumazaki, T. (1992) *Biochem. Biophys. Res. Commun.* 185, 1069–1077.
24. Ricci, G., Lo Bello, M., Caccuri, A. M., Pastore, A., Nuccetelli, M., Parker, M. W., & Federici, G. (1995) *J. Biol. Chem.* 270, 1243–1248.

BI971903G